Kinetic Study of the Reaction of Hydrogen Atoms with Molecular Chlorine at MilliTorr Pressures

Otto Dobis and Sidney W. Benson*

Loker Hydrocarbon Research Institute, University of Southern California, University Park, Los Angeles, California 90089-1661

Received: June 21, 1999; In Final Form: November 9, 1999

The bimolecular reaction H + Cl_2 → HCl + Cl (1) is studied in the very low-pressure reactor (VLPR) system at room temperature. Excellent mass balances are found between the Cl_2 consumption and both HCl as well as Cl product formation. This indicates that only reaction 1 occurs in the system. Its rate constant is $k_1 = (0.96 \pm 0.04) \times 10^{-11}$ cm^3/(molecule·s) at 298 K. Two independent estimates of the *A* factor give a value log A_1(298 K) = −9.80 ± 0.15 (units of cm^3/(molecule·s)). Together with the measured rate constant this yields an activation energy of 1.7 ± 0.2 kcal/mol. All experimental data support a bent transition state for reaction 1.

Introduction

The fast, exothermic reaction

$$H + Cl_2 \rightarrow HCl(v) + Cl + 45.2 \text{ kcal/mol} \qquad (1)$$

has been intensively studied by a number of research workers. It is an integral part of the $H_2 + Cl_2$ chain reaction system and is the pumping stage of the HCl chemical laser.[1] Since the reaction is highly exothermic, HCl can be produced with high vibrational ($v \leq 6$) excitation[2] and an inverted vibrational population. This nonequilibrium energy distribution has been a spur to theoretical studies of the molecular dynamics of this light−heavy−heavy type, exoergic exchange reaction. The fast rate accompanied by this exoergicity presents quite difficult experimental problems, especially in low-pressure, fast flow systems, where the reaction

$$H + HCl(v) \rightarrow H_2 + Cl \qquad (2)$$

enhances the H atom consumption rate and imposes difficult constraints on the usual use of pseudo-unimolecular reaction conditions ($[H]_0 \ll [Cl_2]_0$). In the $H_2 + Cl_2$ chain system, reaction 2 represents a very fast inhibition step. This and some other side processes, like the quenching of HCl(v) and the wall removal of free atoms, further complicate the experimental task. This can be seen In Table 1, where the reported experimental kinetic parameters for reaction 1 are summarized along with some brief characteristics of the experimental systems: H atom generation, input reactant conditions, and analytical method. In spite of the large experimental effort, no easy conclusions can be made from those data. The reported rate constants at room-temperature spread over a factor of 9. The highest values are obtained under $[H]_0 > [Cl_2]_0$ conditions which may indicate some interference by reaction 2. Low values are obtained from relative measurements made in static systems where the perturbation by side reactions is expected to be unimportant. However, the choice of a standard reference, competitive reaction is restricted by the speed of reaction 1. Although the rate constant measurements of the reference reaction show considerable variation, the reason for selecting the data of ref 15 for the absolute rate calculation is that this work measures the thermal rate of reaction 2 at high $[HCl]_0/[H]_0$ ratios using SF_6 as a vibrational quencher. It reproduces the equilibrium constant for Cl + H_2 ↔ HCl + H in satisfactory agreement with thermochemistry[16,17] and gives the exact value of $K_{eq} = 0.27$ in combination with the forward reaction rate[18] at 298 K. The use of an evaluated kinetic expression[19] for a thermal k_2 gives the same k_1 values at room temperature, but higher A_1 values in compensation with a higher E_1.

The different analytical methods used show no correlation with the values of k_1 reported. This suggests that the discrepancies may arise from the fine details of experimental systems and the extent of possible side processes.

Pressure and flow rate variations investigated in the fast flow tube moving inlet experimental test system[23] have resulted in about 25% higher k_1 value with high-pressure turbulent flow than with low-pressure (≤10 Torr) laminar flow measurements (rows 12 and 13 of Table 1). All other discharge flow (DF) measurements shown in Table 1 were carried out at low pressure (1−7 Torr) and at $v = 15-95$ m/s linear flow conditions using $[H] < 10^{12}$ atoms/cm^3 concentrations, where the resonance fluorescence (RF) signal of H atoms is strongly linear with its concentration.[6,7] Since no details of experiments for the H + Cl_2 reaction are available,[23] this observation remains a puzzle.

In our earlier publication[20] we have noted that our H_3PO_4-coated microwave discharge tube produces a small H atom flow which is independent of the applied microwave power. It maintains a low, permanent background H atom concentration, on the order of 10^{10} atoms/cm^3, in the reaction cell which is too small to measure with mass spectrometry at low voltages due to the small ionization cross section of H atoms. It was also shown that the HCl residence time in our reactor cell is more than 20 times longer[21] than the average spontaneous radiative decay time of HCl(v=1). Since the mass spectrometric measurements of Cl_2, Cl, and HCl are well established in our VLPR system,[22] this "invisible" background H atom concentration can be explored by Cl_2 titration under the thermalized conditions of VLPR. As the Cl_2 consumption as well as HCl and Cl product formation rates are measured simultaneously in our system, they can provide pure thermal kinetic information

10.1021/jp9920601 CCC: $19.00
Published on Web 01/06/2000

TABLE 1: Experimental and Theoretical Kinetic Parameters for the Reaction H + Cl_2 → HCl + Cl

T, K	A^a	E_a, cal/mol	$k_{298}{}^a$	system, conditions	anal method	ref
273−335	5.43	1570	0.39	static,	rel to	3
	(9.23)	(1880)	(0.39)	[H(T)Cl/[Cl2] ~ 0.5	H + HCl[b]	
196−296[c]	3.10	1120	0.46	static,	rel to	4
	(5.16)	(1430)	(0.46)	$[HCl]/[Cl_2] = 10-60$	H + HCl[b]	
292−434	7.6 ± 2.1	1420 ± 200	0.70	DF,[d] $[Cl_2] > [H]$	MS of Cl_2, HCl; ESR of H	5
252−458	14.4 ± 2.8	1190 ± 144	1.94	DF,[d] $[Cl_2] \gg [H]$	RF[e] of H	6
300−750	14.1 ± 1.2	1150 ± 129	2.04	DF,[d] $[Cl_2] \gg [H]$	RF[e] of H	7
294−557	62 ± 6	1800 ± 300	3.00	DF,[d] $[H] > [Cl_2]$	MS of H, Cl_2	8
298			1.83	DF,[d] $[Cl_2] > [H]$	esr of H, Cl	9
298			1.70	DF,[d] $[Cl_2] \gg [H]$	RF[e] of H	10
298			2.13	DF,[d] $[Cl_2] \gg [H]$	UV absorbance of H	11
298			1.60	DF,[d] $[Cl_2] > [H]$	RF[e] of H	12
298			3.50	DF,[d] $[H] > [Cl_2]$	MS of Cl_2	13
298			2.0[f]	DF,[d] $[Cl_2] \gg [H]$	RF[e] of H	23
298			1.5[g]	DF[d] $[Cl_2] \gg [H]$	RF[e] of H	23
300			0.39	static,	rel to	14
			(0.39)	$[HCl]/[Cl_2] = 20-120$	H + HCl[b]	
250−730	7.2 ± 0.7	1200 ± 100	0.96[h]			34
298	$(16.0)_{cal}$	$(1680)_{cal}$	0.96 ± 0.04	VLPR, $[Cl_2] > [H]$	MS of Cl_2, Cl, HCl	this work

[a] *A* and *k* are in units of 10^{-11} cm^3/(molecule·s). [b] Absolute values of *A*, *E*, and *k* are calculated using $k_{ref} = (7.8 \pm 1.8) \times 10^{-12} \exp(-3110 \pm 167)/RT$ of ref 15 and $k_{ref} = 1.32 \times 10^{-11} \exp(-3420/RT)$ of ref 10 (in parentheses). [c] Data are limited to three steps of T. [d] DF = discharge flow. [e] RF = resonance fluorescence. [f] Measured with high pressure (60−160 Torr) turbulent flow conditions. [g] Measured with low pressure (2−10 Torr) plug flow conditions. [h] Obtained by ab initio potential energy surface (PES) calculations.

on reaction 1 independently of any possible perturbation from reaction 2 or other side reactions.

Experimental Section and Results

The VLPR system used for current measurements is the same[20,21] three-stage, all-turbo-pumped equipment we have used for all previous experiments. It has been described in detail earlier.[24] However, the system parameters, the present experimental sequence, and data processing are briefly summarized below.

The thin Teflon-coated, cylindrical, thermostated flow cell reactor of volume $V_r = 217.5$ cm^3 is mounted on the top of the main vacuum chamber. Gas inlets are affixed on the top of the reactor preceded by resistive capillary flow subsystems calibrated for regulating the fluxes of initial gas components with the use of Validyne transducers. Two gas inlets are used in the present series of measurements. One of the inlets is connected through the phosphoric acid coated quartz discharge tube centered in the Opthos microwave generator cavity of a McCarrol antenna before joining at the tapered capillary inlet of the reactor cell. This feed-through is used for a 5% Cl_2/He gas mixture inlet flow in the first series and then for a pure He inlet in the second series of runs. The other supply line serves for a 10% Cl_2/He gas mixture inlet flow which provides the Cl_2 reactant concentration for reaction 1 in the reactor cell.

At the bottom of the reactor, the gas escape orifice of 0.277 cm diameter (marked ϕ_3 in our earlier studies) is used. With the above reactor volume V_r, the first-order escape rate constant for any component of mass *M* is given by $k_{eM} = 0.546(T/M)^{1/2}$ s^{-1}, where *T* is the absolute temperature. The reactor cell operates in the Knudsen flow regime. The strictly controlled gas inlet and outlet dynamics establish the well-defined steady state flow conditions in the reactor. The uncertainty in flow is less than 1%.

The gas mixture leaves the reactor cell through the exit orifice in the form of an effusive molecular beam. This beam is chopped by a tuning fork and further collimated by two successive pinholes in the differentially pumped vacuum system to reduce the background mass signal. The beam is sampled with the off-axis mass analyzer of the mass spectrometer and the mass signals are fed to a phase sensitive lock-in amplifier tuned to the chopping frequency. The measured mass ranges are repeatedly scanned, usually 20−30 times to give a good statistical average, and the mass intensities are recorded for data acquisition. Each mass signal is corrected for its small background value recorded prior to start-up of mass flow. The chopping and phase-sensitive detection ensures that we are sampling species which have not made a collision after leaving the reactor.

Mass spectral calibration for a given gas component of mass *M* is carried out by measuring the mass signal intensity I_M as a function of the specific flux *F*(M) according to the relationship $I_M = \alpha_M F(M)$, where α_M is the mass spectral efficiency for mass *M* and $F(M) = \text{flux}/V_r$ in molecules/(cm^3·s) unit. This relationship is strictly linear in the mass flow range used as is shown in Figure 1 for Cl_2 analysis. The steady state concentration of M in the reactor cell then can be calculated from the relation $[M] = F(M)/k_{eM}$.

The mass analyzer is very sensitive for the specific flux of Cl_2. The slopes in Figure 1 give $\alpha_{Cl_2} = (3.018 \pm 0.036) \times 10^{-10}$ with 40 eV and $(1.009 \pm 0.015) \times 10^{-10}$ with 20 eV electron energies. Depending on the electron energy used, Cl_2 undergoes some fragmentation which produces Cl atom signals at masses 35 and 37. This fragmentation ratio is presented in Figure 2 as a function of ionizing potential. The values at the two voltages of kinetic measurements are 0.67×10^{-2} with 20 eV and 3.56×10^{-2} with 40 eV. These ratios are used for making corrections to the mass signals of Cl atoms produced in reaction 1.

In the course of experimental measurements, the Cl_2 flow using a 5% Cl_2/He composition is started first through the newly coated microwave discharge inlet and the mass signal intensities of the Cl_2 isotopes (at 70, 72, and 74 amu) are repeatedly recorded. This flow corresponds to $[Cl_2]_0 = 14.31 \times 10^{11}$ molecules/cm^3 steady state concentration in the reactor cell. Then the microwave generator is turned on and its power is adjusted to total dissociation of Cl_2 observed by the disappearance of Cl_2 mass signals and their replacement by Cl atom and HCl signals. The total balance of Cl_2 decomposed and Cl + HCl formed has been studied in detail earlier using absolute mass signal intensity measurements.[22] The experimentally found mass conservation relations have shown a ±2% scatter at most which sets $\alpha_{Cl} = \alpha_{HCl}$ within the same uncertainty.[22]

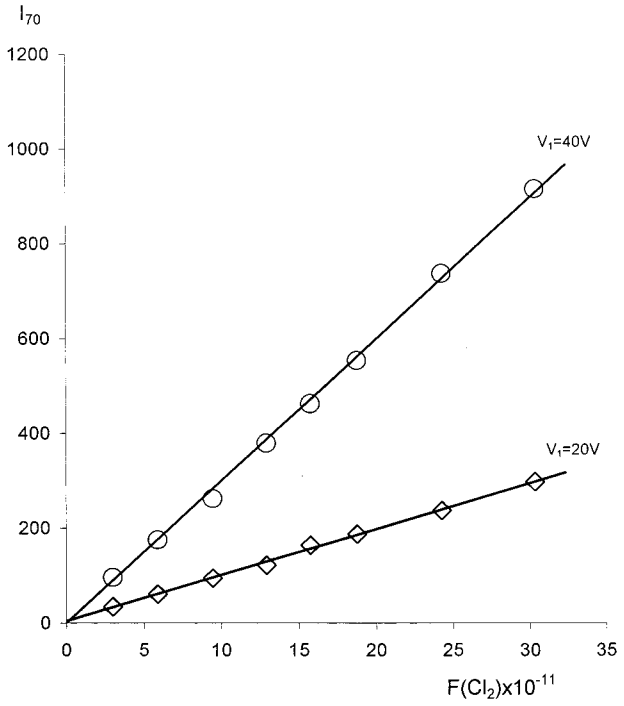

Figure 1. Mass 70 signal intensities (in arbitrary units) of Cl_2 recorded at various specific flow rates of 10.00% Cl_2/He mixture using 20 and 40 V ionization energies.

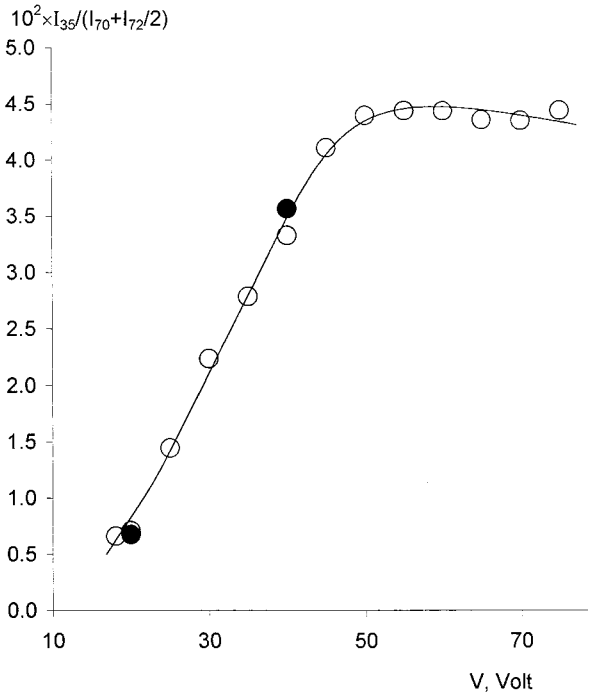

Figure 2. Cl_2 fragmentation (in percentage) as a function of electron energy measured with 1.574×10^{12} molecules/(cm^3·s) specific flow rate of Cl_2. Solid circles represent average values of various flow rate measurements calculated from the data of Figure 1.

There is no Cl but always HCl signal in full mass balance with Cl_2 at the start-up of the microwave generator. Over a 1−2 h period, the Cl/HCl ratio increases until it reaches a permanent value of about 50% which is usually maintained for about 40−50 h which is the service life of the H_3PO_4 coat. In the present case, the permanent ratio of $I_{Cl}/(I_{Cl} + I_{HCl})$ is 0.502 from which the initial steady state Cl concentration is calculated as $[Cl]_0 = 2F(Cl_2)I_{Cl}/(I_{Cl} + I_{HCl})k_{eCl}$. This value, along with $[HCl]_0$, is given in the first part data head of Table 2. Through the separate

TABLE 2: Initial and Final Steady State Concentrations[a] of Cl_2 Reactant and of Cl and HCl Products

		$[Cl]_0 = 10.22$, $[HCl]_0 = 10.16$			$[Cl]_0 = [HCl]_0 = 0$		
no.	$[Cl_2]_0$	$[Cl_2]$	$\Delta[Cl]^b$	$\Delta[HCl]^b$	$[Cl_2]$	[Cl]	[HCl]
1	3.54	2.66	0.67	0.70	2.68	0.61	0.63
2	5.16	4.00	0.83	0.85	4.00	0.79	0.81
3	7.70	6.16	1.11	1.08	6.16	1.01	1.05
4	10.63	8.71	1.45	1.36	8.65	1.35	1.35
5	16.66	14.24	1.66	1.66	14.48	1.69	1.70
6	21.62	18.90	1.85	1.89	18.56	1.89	1.88
7	27.09	24.12	1.97	2.01	24.10	2.11	2.10

[a] All concentrations are in units of 10^{11} particles/ cm^3. [b] $\Delta[X] = [X] - [X]_0$, where X = Cl or HCl.

supply line, a gradually increasing flow of the 10% Cl_2/He gas composition can be introduced which corresponds to the Cl_2 initial concentrations given in the second column of Table 2. The actual concentration of Cl_2 as well as the increases in Cl and HCl concentrations were measured in each step. Because of a relatively large HCl concentration, corrections for HCl fragmentation[24] were also made to the Cl atom signals.

After the Cl_2 gas composition in the microwave discharge line was replaced by pure He flow, the whole procedure was repeated with the same steps of $[Cl_2]_0$, but with zero $[Cl]_0$ and $[HCl]_0$ initial concentrations. These results are given in the second part of Table 2.

The amounts of Cl and HCl products formed in reaction 1 are equal within an average ±2% scatter and are independent of their initial values as shown in Table 2. On combining the steady state kinetic equations for Cl_2 consumption with those for formation of Cl or HCl, the kinetic mass balance gives the following equalities:

$$\Delta[Cl_2]k_{eCl_2} = \Delta[Cl]k_{eCl} = -\Delta[HCl]k_{eHCl} \qquad (3)$$

where $\Delta[Cl_2] = [Cl_2]_0 - [Cl_2]$. This balance is shown in Figure 3 indicating that the Cl_2 reactant consumption and product recovery according to reaction 1 is better than 97% in our experimental system. Note that these equalities rule out any loss of HCl by wall reactions or production of Cl by reaction 2.

With the single reaction 1 established, the steady state H atom consumption kinetics is given by

$$([H]_0 - [H])k_{eH} = k_1[H][Cl_2]$$

Upon substituting $k_1[H][Cl_2] = \Delta[Cl]k_{eCl}$ from the steady state kinetics of Cl formation and $[H] = \Delta[Cl_2]k_{eCl2}/k_1[Cl_2]$ from the steady state kinetics of Cl_2 consumption, we obtain

$$\frac{\Delta[Cl_2]}{[Cl_2]} = \frac{k_1}{k_{eCl_2}}[H]_0 - \frac{k_1 k_{eCl}}{k_{eH}k_{eCl_2}}\Delta[Cl] \qquad (4)$$

which is a convenient form to determine both k_1 and $[H]_0$ values. Plotting values of $\Delta[Cl_2]/[Cl_2]$ against $\Delta[Cl]$ according to eq 4, a good linear relationship, presented in Figure 4, is obtained, where rate constant $k_1 = (0.96 \pm 0.04) \times 10^{-11}$ cm^3/(molecule·s) is calculated from the slope, and $[H]_0 = (4.85 \pm 0.11) \times 10^{10}$ atoms/cm^3 is found from the ratio of intercept to slope.

Discussion

The presence of background hydrogen in kinetic systems using microwave or RF discharge H atom generation is well-known. With $[H]_0 \ll [Cl_2]_0$ conditions, a low permanent inlet concentration of hydrogen, usually $[H]_o \leq 10^{12}$ atoms/cm^3, can be maintained by the microwave decomposition of impurities

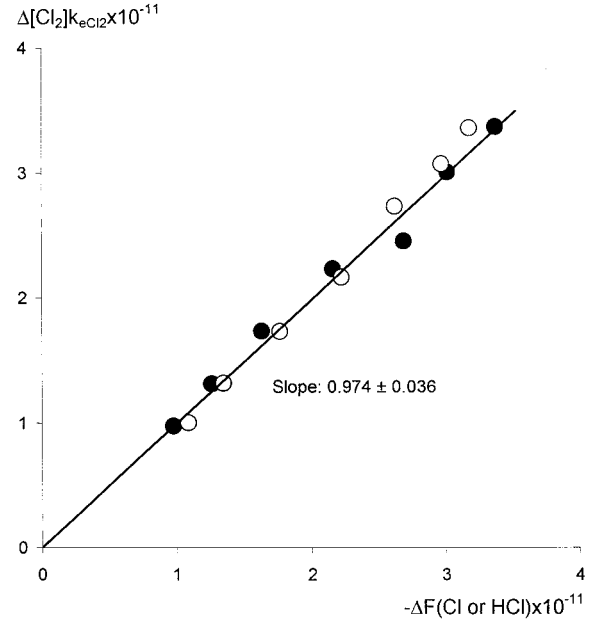

Figure 3. Mass flow balance between Cl_2 consumption and Cl atom or HCl formation rates in the H/Cl_2 two-component system plotted according to eq 3. Solid circles represent the measurements with pure He flow in the discharge tube (microwave on), while open circles denote measurements started with initial conditions of $[Cl]_0 = (10.22 \pm 0.21) \times 10^{11}$ and $[HCl]_0 = (10.16 \pm 0.25) \times 10^{11}$ molecules/cm^3.

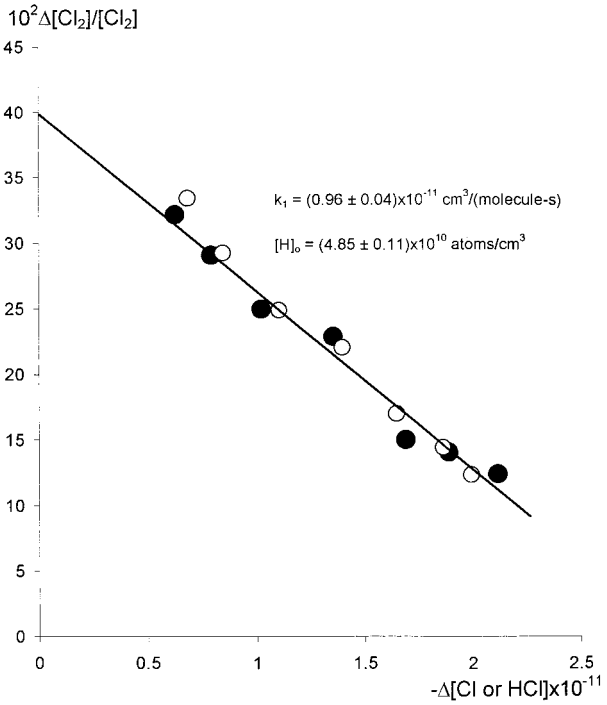

Figure 4. Relative Cl_2 consumption versus Cl or HCl formation rates plotted according to eq 4. The slope and intercept are proportional to k_1 and $[H]_0$, respectively. Symbols of measurements are the same as in Figure 3.

(mostly water) of the carrier gas[7,10,23] He or Ar. In our system this background hydrogen content can be well measured by Cl_2 titration according to reaction 1. Because of the nature of the VLPR system as used here, both the steady state initial concentration of the hydrogen atom and rate constant k_1 can be determined in one series of experiments. This is a consequence of the fact that, although the ratio of initial concentrations $[Cl_2]_0/[H]_0$ varies between 7 and 56, the kinetics can still be measured under real second-order conditions using absolute concentration measurements. This is in sharp contrast with the moving inlet flow systems, where under such initial conditions, pseudo-first-order kinetics is employed.

The kinetic balance of Cl_2 consumption and product formations expressed by eq 3 indicates that no wall removal of free atoms exists in our system. The experimental evidence for the absence of Cl atom wall recombination is the complete dissociation of Cl_2 achieved by microwave discharge. Theoretically, there are three kinds of atom removal to be considered in the H/Cl_2 reaction system:

$$2Cl \rightarrow Cl_2 \qquad \text{(w1)}$$

$$H + Cl \rightarrow HCl \qquad \text{(w2)}$$

$$2H \rightarrow H_2 \qquad \text{(w3)}$$

Reaction w1 is the fastest one and should be accounted for in all cases when $[Cl_2] \leq [H]$. Ambridge et al.[5] have included this surface reaction in their kinetic scheme. Reaction w2 is considered to be fast[25] and should be taken into account when $[Cl_2] \gg [H]$, that is, when the kinetics is measured by the loss of H atoms. Wagner et al.[6] neglected this surface reaction which they justified by referring to the direct measurements of Spencer and Glass.[26] But the low k_w value in the reaction system of Spencer and Glass is due to the applied halocarbonwax coat. This may hint some overshoot in the reported[6] k_1 value. Similarly, the observed wall reaction rates of refs 7 and 12 can be attributed to reaction w2. The same experimental system used by Michael et al.[12] shows no wall removal of H atom by reaction w3 when it is used for the chlorine-free kinetic study of the $H + C_2H_4 \rightarrow C_2H_5$ reaction.[27] In any case, when surface reaction w1 is observed, (w2) should also be taken into account, but it was omitted from the overall mechanism of Ambridge et al.[5]

In our Teflon-coated reactor cell, surface reactions w1 and w2 would conflict with the linear relationships shown in Figures 3 and 4. Only the hypothetical, sole existence of reaction w3 would still preserve these linear relationships, not changing eq 3, but altering eq 4 to

$$\frac{\Delta[Cl_2]}{[Cl_2]} = \frac{k_1}{k_{eCl_2}}[H]_i - \frac{k_1 k_{eCl}}{k_{eCl_2}(k_{eH} + k_{w3})}\Delta[Cl] \qquad (5)$$

where $[H]_i = [H]_o k_{eH}/(k_{eH} + k_{w3})$. Equation 5 would lead to higher k_1 values and to lower values of $[H]_0$. In our VLPR system the absence of surface reaction w3 was tested earlier[28] using the same Teflon-coated reactor cell and different exit orifice sizes. Surface reaction w3 is the most unlikely process in any H/Cl_2 experimental system. None of the studies compiled in Table 1 have considered it. In our system, wall reaction w3 would be expected to be accompanied by wall reaction w2. This would upset the flow balance given by eq 3, especially in the first series of runs, where high initial Cl concentration is used.

Regardless of the Cl_2/H ratio, there are no wall reactions w1−w3 observed when the reactor surface is coated with boric acid,[8] phosphoric acid,[10,11] halocarbonwax,[23] or treated with HF.[13]

The sole existence of reaction 1 in our system is indicated by the experimentally well-established mass balance expressed by eq 3 and presented in Figure 3. Two earlier publications[5,13] examined the experimental mass balances in the $H + Cl_2$ reaction system. Ambidge et al.[5] found that the $\Delta[H]/\Delta[Cl_2]$ ratio decreases with increasing $[Cl_2]_0/[H]_0$ and approaches 2 asymptotically, while $\Delta[HCl]/\Delta[H]$ increases with the same ratio of reactants and approaches 1, but no Cl atom product was detected. With high initial ratios of reactants $[Cl_2]_0/[H]_0$, these

results lead to a chlorine balance: $2\Delta[Cl_2] = \Delta[HCl]$. Assuming a reaction mechanism which consists of reactions 1 and 2, the total wall recombination of Cl, and the homogeneous quenching of HCl(v) with Cl_2, a varying H atom consumption stoichiometry was deduced.[5] Its value changes from 1 to 2 with increasing $[Cl_2]_0/[H]_0$. The problem with this mechanism is that the quenching of HCl(v) with Cl_2 is a very slow process[29] (about 4 orders of magnitude slower than with H atom), and therefore its rate is insignificant in the 1−8 ms reaction time scale. It will not establish a steady state HCl(v) concentration in competition with reaction 2 as claimed by the authors.[5]

Stedman et al.[13] found a consumption balance of reactants $\Delta[H] + \Delta[H_2] = \Delta[Cl_2]$, where the H_2 consumption arises from the reaction of vibrationally excited hydrogen:

$$Cl + H_2(v) \rightarrow HCl + H \qquad (6)$$

This reaction is exothermic for $v \geq 1$, and it becomes the H atom chain recovery step of the entire mechanism with an estimated rate constant[13,19] of $k_6 \sim 1.5 \times 10^{-12}$ cm^3/(molecule·s) for $H_2(v=1)$ reaction. Active $H_2(v)$ is formed in the microwave or RF discharge process[30] by partial excitation of ground electronic state H_2. Its concentration may be as high as 15% of the total H_2 passed through the microwave discharge area.[13] Considering the Cl atom removal, reaction 6 is now indistinguishable from the wall recombination of Cl. Since the only effective quencher in these fast flow systems is product HCl, the overall mechanism is further complicated by

$$H_2(v) + HCl \rightarrow HCl(v) + H_2 \qquad (7)$$

an energy transfer process which then enhances reaction 2. The known rate constant[31] of reaction 2 involving HCl($v=1$) as excited reactant is 7×10^{-12} cm^3/(molecule·s) and 4 times higher[32] with HCl($v=2$) as reactant. Higher excitations ($v > 2$) would further increase the rate of reaction 2 and, with the contribution of energy transfer process 7, it may become a moderate side process for H atom consumption especially under $[H]_0 \sim [Cl_2]_0$ conditions.

Because of the fast rate of reaction 1, all discharge flow systems have to use fast linear flow velocities (∼15−95 m/s) and short injector position displacement (∼1−15 cm) to ensure a short contact time (∼1−15 ms). In this short time scale the perturbations by reactions 2, 6, and 7, as well as the mixing time of reactants, should be taken into account. These experimental difficulties, together with the lack of a clear-cut reaction mechanism, may lead to those large discrepancies presented in Table 1 in the kinetic investigations of this apparently simple elementary reaction. In comparison, the long residence time (0.6−0.9 s) of the VLPR system ensures thermalized conditions and the excellent mass balance of Cl_2 consumption with Cl and HCl product formation indicate the sole existence of reaction 1 in our system.

The exoergic character of reaction 1 has attracted a number of authors to perform ab initio potential energy surface (PES) calculations. High-level, large basis set computations of the barrier height[33] support a 1.40−1.45 kcal/mol activation energy with collinear or slightly bent (170°) transitions state (TS) configuration. They also reproduce the exoergicity of the reaction within ±1 kcal/mol. With similar PES and London−Eyring−Polanyi−Sato (LEPS) empirical surface calculations, Gonzales et al.[34] have computed thermal rate constants for reaction 1 using the variational transition state theory with semiclassical tunneling corrections. They found a satisfactory

TABLE 3: Transition State Entropy Calculation for the *A* Factor of Reaction 1 Using H + Cl_2 ↔ [HSCl]‡ Model Reaction[a]

partial contributions (eu)	$\Delta_{298}S_p^{\ddagger}$ (bent, 120°)
model reaction	−27.1
translation	0.4
spin, electronic	1.4
rotation	0.6
S−Cl, stretch (565 cm^{-1}), RC	−0.6
H·S, stretch (1800 cm^{-1})	0.0
H·S·Cl, bend (900 → 500 cm^{-1})	0.5
total	−18.8

[a] Entropy of HSCl (S°_{model} = 59.6 eu) is calculated by bond additivity[37] according to $^1/_2H_2S + {}^1/_2SCl_2$ ↔ HSCl isodesmic,hypothetical reaction. [b] RC = reaction coordinate.

TABLE 4: Transition State Entropy Calculation for the *A* Factor of Reaction 1 Using H + Cl_2 ↔ $[Cl_2]^{\ddagger}$ Model Reaction

partial contributions (eu)	$\Delta_{298}S_p^{\ddagger}$ (bent, 120°)
model reaction	−27.4
translation	0.1
spin, electronic	1.4
symmetry	1.4
rotation (2-D)	0.7
rotation (1 − *D*)	5.3
Cl−Cl, stretch (565 cm^{-1}), RC[a]	−0.6
H·Cl·Cl, bend (900 → 500 cm^{-1})	0.5
H·Cl, stretch (2000 cm^{-1})	0.0
total	−18.6

[a] RC = reaction coordinate.

linear Arrhenius function

$$k_1 = (7.2 \pm 0.7) \times 10^{-11} \exp(-1200 \pm 100)/RT \qquad (8)$$

between 252 and 730 K based on optimized PES calculation (*RT* in cal/mol). This would exactly reproduce our experimental rate constant at 298 K, although we have some reservations concerning the steep angular dependence of the TS energy barrier. It starts from a very low barrier at collinear TS geometry (Table 4 of ref 31). This function is remarkably different from those obtained with LEPS[33] or semiempirical "diatomics-in-molecule" PES calculation.[35] The reaction free-energy criterion used in the canonical variation theory imposes a compensation[36] between the Arrhenius parameters when applied to thermal rate constant calculations.

A reliable empirical approximation of the experimental A_1 factor can be performed by estimating the entropy of activation $\Delta S^{\ddagger}$ using the entropy change of a suitable model reaction and correcting it with partial entropy contributions for perturbations and changes in the degrees of freedom:[37]

$$\Delta S^{\circ\ddagger} = (S^\circ_{model} - S^\circ_{H} - S^\circ_{Cl_2}) + \sum \Delta S^\circ(\text{corrections}) \qquad (9)$$

where

$$\sum \Delta S^\circ(\text{corrections}) = \Delta S^\circ(\text{transl}) + \Delta S^\circ(\text{rot}) + \Delta S^\circ(\text{vib}) + \Delta S^\circ(\text{electronic}) + \Delta S^\circ(\text{symmetry}) \qquad (10)$$

The right side terms of eq 10 can be calculated using known thermochemical functions.[37] The results of such calculations are summarized in Table 3 using the hypothetical model reaction H + Cl_2 → [HSCl]‡, and in Table 4 using an H atom insertion model reaction H + Cl_2 → $[Cl_2]^{\ddagger}$. Summing up the partial

contributions for corrections, the two model calculations give the TS entropy change in good agreement.

Correcting the overall entropy change in Tables 3 and 4 from pressure to concentration unit, $A_1 = (1.60 \pm 0.48) \times 10^{-10}$ cm^3/(molecule·s) is obtained. It is more than twice the value derived from ab initio calculations in eq 8, but in good agreement with the experimental values of refs 6 and 7. This A_1 factor and the measured k_1 rate constant yields the activation energy $E_1 = 1.68 \pm 0.18$ kcal/mol which is in good agreement with the activation energies in Table 1. Empirically estimated A factors computed by the above methods have never shown discrepancies greater than a factor of 2 and we estimate the uncertainty as a factor of 1.5 leading to the uncertainties listed above.

A linear model of the TS would lead to a replacement of the rotational mode by a doubly degenerated bending mode at about 500 cm^{-1}, yielding an A factor 10-fold smaller, $A_1 = 1.6 \times 10^{-11}$ cm^3/(molecule·s). The activation energy would than be 0.28 kcal/mol. Both A_1 and E_1 are well below all of the values measured and would seem to rule out a linear transition state.

Conclusions

A low, permanent H atom inlet flow is produced by the operation of the phosphoric acid coated microwave discharge tube of the VLPR system. This background $[H]_0$ concentration in the system can be determined by Cl_2 titration.

An excellent balance is found between the Cl_2 consumption and the Cl as well as the HCl formation kinetics under steady state flow conditions. It indicates the sole existence of reaction 1 in our system without any perturbation from reactions of vibrationally excited secondary products. This is due to the relatively long residence time in the reactor cell which allows the thermalization of HCl(v). Since the kinetic investigation is performed under real second-order kinetics, both the rate constant and the initial H atom concentration can be determined in one series of measurements as $k_1 = (0.96 \pm 0.04) \times 10^{-11}$ cm^3/(molecule·s) and $[H]_0 = (4.85 \pm 0.11) \times 10^{10}$ atoms/cm^3. Both values are independent of the initial Cl and HCl concentrations.

Acknowledgment is made to the donors of the Petroleum Research Fund administered by the American Chemical Society, for the support of this research.

References and Notes

(1) Cohen, N.; Jacobs, T. A.; Emanuel, G.; Wilkins, R. L. *Int. J. Chem. Kinet.* **1969**, *1*, 551.
(2) Anlauf, K. G.; Horne, D. S.; Macdonald, R. G.; Polanyi, J. C.; Woodall, K. B. *J. Chem. Phys.* **1972**, *57*, 1561.
(3) Klein, F. S.; Wolfsberg, M. *J.Chem. Phys.* **1961**, *34*, 1494.
(4) Davidov, R. S.; Lee, R. A.; Armstrong, D. A. *J. Chem. Phys.* **1966**, *45*, 3364.
(5) Ambidge, P. F.; Bradley, J. N.; Whytock, D. A. *J. Chem. Soc., Faraday Trans. 1* **1976**, *72*, 1157.
(6) Wagner, H. G.; Welzbacher, U.; Zellner, R. *Ber. Bunsen-Ges. Phys. Chem.* **1976**, *80*, 902.
(7) Bemand, P. P.; Clyne, M. A. A. *J. Chem. Soc., Faraday Trans. 2* **1977**, *73*, 394.
(8) Dodonov, A. F.; Lavrovskaya, G. K.; Morozov, I. I.; Ulbright, R. T.; Tal'roze, V. L.; Lyubimova, A. K. *Kinet. Catal.* **1970**, *11*, 677. Albright, R. G.; Dodonov, A. F.; Lavrovskaya, G. K.; Morosov, I. I.; Tal'roze, V. L. *J. Chem. Phys.* **1969**, *50*, 3632.
(9) Bykhalo, I. B.; Filatov, V. V.; Gordon, E. B.; Perminov, A. P. *Russ. Chem. Bull.* **1994**, *43*, 1637.
(10) Kita, D.; Stedman, D. H. *J. Chem. Soc., Faraday Trans. 2* **1982**, *78*, 1249.
(11) Jaffe, S.; Clyne, M. A. A. *J. Chem. Soc., Faraday Trans. 2* **1981**, *77*, 531.
(12) Michael, J. V.; Lee, J. H. *Chem. Phys. Lett.* **1977**, *51*, 303.
(13) Stedman, D. H.; Steffenson, D.; Niki, H. *Chem. Phys. Lett.* **1970**, *7*, 173.
(14) Jardine, D. K.; Ballash, N. M.; Armstrong, D. A. *Can. J. Chem.* **1973**, *51*, 656.
(15) Ambidge, P. F.; Bradley, J. N.; Whytock, D. A. *J. Chem. Soc., Faraday Trans. 1* **1976**, *72*, 2143.
(16) Weston, E. R. *J. Phys. Chem.* **1979**, *83*, 61.
(17) Miller, J. C.; Gordon, R. J. *J. Chem. Phys.* **1981**, *75*, 5305.
(18) Benson, S. W.; Cruickshank, F. R.; Shaw, R *Int. J. Chem. Kinet.* **1969**, *1*, 29.
(19) Baulch, D. L.; Duxbury, J.; Grant, S. J.; Montague, D. C. *J. Chem. Phys. Ref. Data* **1981**, *10*, 1, Suppl.1.
(20) Dobis, O.; Benson, S. W. *J. Phys. Chem.* **1997**, *101*, 1305 (Table 1).
(21) Dobis, O.; Benson, S. W. *J. Phys. Chem.* **1995**, *99*, 4986.
(22) Dobis, O.; Benson, S. W. *J. Am. Chem. Soc.* **1991**, *113*, 6377.
(23) Seeley, J. V.; Jayne, J. T.; Molina, M. J. *Int. J. Chem. Kinet.* **1993**, *25*, 571.
(24) Dobis, O.; Benson, S. W. *Int. J. Chem. Kinet.* **1987**, *19*, 691.
(25) Galante, J. J.; Gislason, E. A. *Chem. Phys. Lett.* **1973**, *15*, 231.
(26) Spencer, J. E.; Glass. G. P. *J. Phys. Chem.* **1975**, *79*, 2329.
(27) Barker, J. R.; Kiel, D. G.; Michael, J. V.; Osborne, D. T. *J. Chem. Phys.* **1970**, *52*, 2079.
(28) Mitchell, T. J.; Gonzales, A. C.; Benson, S. W. *J. Phys. Chem.* **1955**, *99*, 16960. Vasileides, S.; Benson, S. W. *Int. J. Chem. Kinet*. **1997**, *29*, 915.
(29) Leone, S. R. *J. Phys. Chem. Ref. Data* **1982**, *11*, 953.
(30) Polanyi, J. C.; Sadowski, C. M. *J. Chem. Phys.* **1962**, *36*, 2239. Heidner III, R. F.; Kasper, J. V. V. *J. Chem. Phys.* **1969**, *51*, 4163.
(31) Arnoldi, D.; Wolfrum, J. *Ber. Bunsen-Ges. Phys. Chem.* **1976**, *80*, 892.
(32) Macdonald, R. G.; Moore, C. B. *J. Chem. Phys.* **1980**, *73*, 1681.
(33) Vincent, M. A.; Connor, J. N. L.; Gordon, M. S.; Schatz, G. C. *Chem. Phys. Lett.* **1993**, *203*, 415. Wisscher, L.; Dyall, K. G. *Chem. Phys. Lett*. **1995**, *239*, 181.
(34) Gonzales, M.; Hijazo, J.; Novoa, J. J.; Sayos, R. *J. Chem. Phys.* **1998**, *108*, 3168.
(35) Levine, R. D.; Bernstein, R. B. *Molecular Reaction Dynamics and Chemical Reactivity*; Oxford University Press: New York, 1987; p 141.
(36) Truhlar, D. G.; Garrett, B. C. *Acc. Chem. Res.* **1980**, *13*, 440.
(37) Benson, S. W. *Thermochemical Kinetics*, 2nd ed.; Wiley: New York, 1976; pp 37, 151.